CHEMISTRY
A EUROPEAN JOURNAL

DOI: 10.1002/chem.200700494

The First Open-Paddlewheel Structures in Diruthenium Chemistry: Examples of Intermediate Magnetic Behaviour between Low and High Spin in Ru_2^{5+} Species

M. Carmen Barral,[a] Teresa Gallo,[a] Santiago Herrero,[a] Reyes Jiménez-Aparicio,*[a] M. Rosario Torres,[b] and Francisco A. Urbanos[a]

In memory of Professor F. Albert Cotton

Abstract: The reaction of $[Ru_2Cl(O_2CMe)(DPhF)_3]$ (DPhF = *N*,*N*′-diphenylformamidinate) with aqueous HCl leads to the substitution of the acetate ligand to give the complex $[Ru_2Cl_2(DPhF)_3]$ (**1**). Similar reaction of $[Ru_2(O_2CMe)(DPhF)_3(H_2O)]BF_4$ with aqueous HBr or HI produces $[Ru_2Br_2(DPhF)_3]$ (**2**), and $[Ru_2I_2(DPhF)_3]$ (**3**), respectively. The reaction of **1** with $AgBF_4$ to form the highly unsaturated unit $[Ru_2(DPhF)_3]^{2+}$, which is isolated as $[Ru_2(BF_4)(DPhF)_3(H_2O)]BF_4$ (**4**), and $[Ru_2(MeCN)_2(DPhF)_3](BF_4)_2$ (**5**), is also reported. The use of $AgNO_3$ instead of $AgBF_4$ leads to $[Ru_2(NO_3)_2(DPhF)_3]$ (**6**). The magnetic behaviour of complexes **1**–**4** and **6** is intermediate between high- and low-spin configurations. A relationship between the magnetic behaviour and the visible-near-infrared (Vis-NIR) spectra is apparent. In addition, the crystal structure determinations of **2**, **4**·THF, and **6**, have been carried out. Complexes **1**–**3**, **5** and **6** are the first examples of open-paddlewheel structures in diruthenium chemistry. The BF_4^- bridging the metal centres in **4**·THF is activated and forms very short Ru–F bonds.

Keywords: magnetic properties · multiple bonds · ruthenium · spin states

Introduction

Since the structural determination of $[Re_2Cl_8]^{2-}$ in 1964, which was decisive in establishing the existence of multiple bonds between metal atoms,[1] numerous complexes with the same tetragonal prismatic structure, $[M_2X_8]^{n-}$ (Figure 1a), have been found for Mo, W, Tc, Re and Os. Surprisingly, this structure remains unknown for Ru. Although a huge number of complexes containing Ru_2^{4+}, Ru_2^{5+} and Ru_2^{6+} units have been described, the majority of them show the paddlewheel structure (Figure 1b) in which four bidentate, mononegative, three-atom bridging ligands support the metal–metal bond.[2] These complexes may have two, one or no additional axial ligand. Open-paddlewheel structures (Figure 1c) have been described for several dimetallic com-

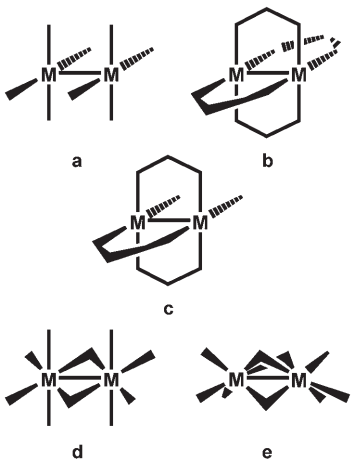

Figure 1. Some structures found in dimetallic complexes.

[a] Dr. M. C. Barral, T. Gallo, Dr. S. Herrero, Dr. R. Jiménez-Aparicio, Dr. F. A. Urbanos
Departamento de Química Inorgánica
Facultad de Ciencias Químicas
Universidad Complutense de Madrid
Ciudad Universitaria, 28040 Madrid (Spain)
Fax: (+34) 91-394-4352
E-mail: reyesja@quim.ucm.es

[b] Dr. M. R. Torres
Centro de Asistencia a la Investigación de Rayos X
Facultad de Ciencias Químicas
Universidad Complutense de Madrid
Ciudad Universitaria, 28040 Madrid (Spain)

pounds, however, none of the diruthenium complexes known to date contain halides or other terminal monodentate ligands at the equatorial positions.

One possible explanation is the lack of stability of the bond Ru equatorial ligand, although the possibility that other dispositions such as face-sharing or even edge-sharing structures are preferred (Figures 1d and e) seems to be more likely.

Recently, we have shown a clean substitution of the acetate ligand in $[Ru_2Cl(O_2CMe)(DPhF)_3]$ (DPhF = *N*,*N*′-diphenylformamidinate) by mono- or polycarboxylic acids under mild conditions.[3,4] Herein, we report the use of hydracids at room temperature to prepare the first diruthenium compounds with monodentate equatorial ligands: $[Ru_2X_2(DPhF)_3]$ (X = Cl, Br, I). In addition, we describe the elimination of the equatorial chloride ligands to give the unsaturated unit $[Ru_2(DPhF)_3]^{2+}$, which is stabilised by the coordination of groups such as BF_4^-, MeCN, or NO_3^-.

Magnetism in Ru_2^{5+} chemistry is another relevant aspect. It is known[5] that in these systems the separation and energy order of π^* and δ^* orbitals lead to different ground and excited terms. The most usual situation derives from the ground state $^4A_2$, which could be the result of the order $\pi^*\delta^*$ or $\delta^*\pi^*$ with a small energy separation between both orbitals. Moreover, a large gap between π^* and δ^* orbitals may generate two different low-spin configurations, $(\pi^*)^3$ or $(\delta^*)^2(\pi^*)^1$, both with a ground term ^2E_g. As a consequence, it is possible to find different magnetic behaviour, low and high spin, and even intermediate situations which must be associated with changes in the electronic spectra of the compounds. Complexes with the framework $[Ru_2(DPhF)_3]^{2+}$ present a rich variety of magnetic properties depending on the axial or equatorial ligands,[3,4,6,7] the counterion in the ionic species,[8] or even the solvent of crystallisation.[8] An analysis of the electronic transitions of this type of complex in the visible-near-infrared region allows us to perceive a relationship between the electronic spectra and their magnetic behaviour.

Results and Discussion

Preparation of the complexes: The acetate ligand in $[Ru_2Cl(O_2CMe)(DPhF)_3]$ is readily replaced by other carboxylates in refluxing MeOH.[3,4] Surely, the use of carboxylic acids with more acidic character than acetic acid would promote the replacement of the acetate group by other carboxylate ligands. Thus, the strongly acidic character of aqueous HCl is sufficient, even at low concentrations, to drive the substitution of the carboxylate by a chloride ligand to form $[Ru_2Cl_2(DPhF)_3]$ (**1**), a new type of complex in ruthenium chemistry (Scheme 1). The same result can be obtained by the reaction of $[Ru_2Cl(O_2CMe)(DPhF)_3]$ with diluted H_2SO_4 in the presence of LiCl. The bromido and iodido derivatives, $[Ru_2Br_2(DPhF)_3]$ (**2**) and $[Ru_2I_2(DPhF)_3]$ (**3**), are obtained from the reaction of $[Ru_2(O_2CMe)(DPhF)_3(H_2O)]BF_4$[7] with aqueous HBr and HI, respectively.

Crystals of **2** are obtained when MeOH is layered in the air over a solution of **2** in CH_2Cl_2. However, when a solution of **2** in chloroform is layered with diethyl ether the colour of the solution slowly changes with time from violet to greenish-brown, showing the decomposition of the complex. However, this transformation was not observed when MeOH/CH_2Cl_2 were used as solvents.

Chloride ligands can be easily removed from **1** by reaction with $AgBF_4$ in a molar ratio 1:2, to give the unsaturated species $[Ru_2(DPhF)_3]^{2+}$, which can be crystallised from THF/hexane or MeCN/Et_2O as $[Ru_2(BF_4)(DPhF)_3(H_2O)]BF_4$·THF (**4**·THF) and $[Ru_2(DPhF)_3(MeCN)_2](BF_4)_2$ (**5**), respectively. Analogously, the reaction of **1** with $AgNO_3$ instead of $AgBF_4$ leads to $[Ru_2(NO_3)_2(DPhF)_3]$ (**6**).

Hence, the $[Ru_2(DPhF)_3]^{2+}$ group is preserved in the reaction of $[Ru_2Cl(O_2CMe)(DPhF)_3]$ or $[Ru_2(O_2CMe)(DPhF)_3(H_2O)]BF_4$ with HX (X = Cl, Br, I) in MeOH. Moreover, when the chloride ligands of complex **1** are removed, species such as MeCN, NO_3^-, or even BF_4^- are sufficient to stabilise the $[Ru_2(DPhF)_3]^{2+}$ unit. However, CH_2Cl_2 and $CHCl_3$ solu-

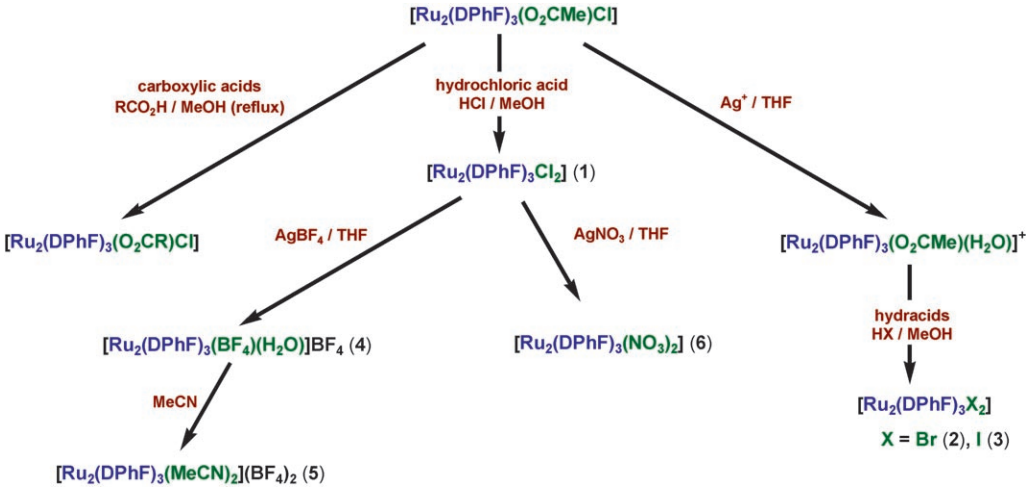

Scheme 1. Reaction pathways involving the trisformamidinate complexes.

tions of **1**–**3** exposed to air show signs of decomposition with time.

IR spectra: The absorptions due to the formamidinate ligands in the IR spectra of **1**–**3** are essentially the same as those observed for other tris(diphenylformamidinato) complexes[4] of Ru_2^{5+}. The only exception is the shift of the band which appears at 1534 cm^{-1} (ν(C=N)) in the starting material to 1525, 1521, and 1519 cm^{-1} for **1**, **2**, and **3**, respectively.

For complexes **4**·THF and **5**, the characteristic wide band at 1060 cm^{-1} due to the BF_4^- groups is observed. Compound **5** presents very weak absorptions at 2314, 2295, and 2277 cm^{-1} owing to the ν(C≡N) vibration of the MeCN ligands. The frequency and intensity of the band assigned to the ν(C=N) vibration of the formamidinate ligands[4] are sensitive to the nature of the equatorial ligands that complete the coordination of the ruthenium atoms in the fragment $[Ru_2(DPhF)_3]^{2+}$. The ν(C=N) vibration absorbs at 1522 cm^{-1} for **4**·THF, which is similar to the value observed for complexes **1**–**3**, although the band is less intense. Notably, halide ligands complete the equatorial positions of the fragment $[Ru_2(DPhF)_3]^{2+}$ in complexes **1**–**4**. However, the ν(C=N) band appears at 1533 cm^{-1} for **5**, the same frequency registered for $[Ru_2Cl(DPhF)_4]$, but higher than the 1526 cm^{-1} observed in $[Ru_2(DPhF)_4(H_2O)]BF_4$.[8] The IR spectrum of **6** shows the set of bands characteristic of the unit $[Ru_2(DPhF)_3]^{2+}$ in addition to several absorptions at 1384, 1237, and 996 cm^{-1} attributed to the nitrate ligands. Probably, the band observed at 1520 cm^{-1} is the sum of two absorptions: ν(C=N) and ν(N=O). Despite the use of acids, none of the complexes shows bands associated with N–H bonds in their spectra.

Magnetic properties and visible-near-infrared spectra: The magnetic moment at room temperature of complexes **1**–**4** and **6** varies from 2.54 to 3.78 BM. These values correspond to an intermediate situation between one and three unpaired electrons, which confirms the complexity of the magnetic behaviour in Ru_2^{5+} compounds with formamidinate ligands.[3,4,6–9] The plot of μ_{eff} versus temperature of complexes **1**–**4** and **6** is depicted in the Figure 2. The corresponding curves of the compounds[4] $[Ru_2Cl(O_2CMe)(DPhF)_3]$ (high spin) and $[Ru_2(NCS)(O_2CMe)(DPhF)_3]$ (low spin) are also presented for comparison. In the series $[Ru_2X_2(DPhF)_3]$ (X = Cl (**1**), Br (**2**), I (**3**)), the room-temperature magnetic moments increase from Cl to I, but in all cases they are intermediate between one and three unpaired electrons in all temperature ranges. However, at low temperature the values for **1** and **2** are close to those corresponding to an $S = 1/2$ spin system. The shape of the curve for complex **1** is very similar to that described for $[Ru_2(O_2CMe)(DPhF)_3(H_2O)]BF_4 \cdot 0.5\,CH_2Cl_2$, which was attributed to a quantum mechanical spin admixture.[7] The magnetic moment curves for **2** and **6** are virtually the same as that for $[Ru_2Cl(Dp\text{-}AniF)_4]$ (Dp-AniF = *N*,*N*′-bis(*p*-anisyl)formamidinate) for which a Boltzmann distribution was proposed.[9] Complex **3** shows a magnetic moment at room temperature that could be associated with three unpaired electrons. However, its magnetic moment decreases continuously with temperature to reach values typical of low-spin complexes at very low temperatures.

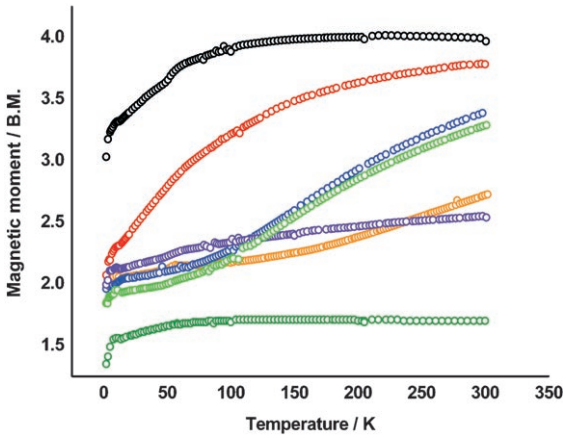

Figure 2. Variable-temperature magnetic moment of $[Ru_2Cl(O_2CMe)(DPhF)_3]$ (black), complex **1** (orange), **2** (blue), **3** (red), **4**·THF (violet), **6** (green) and $[Ru_2(NCS)(O_2CMe)(DPhF)_3]$ (olive).

Complex **4** shows magnetic moment values close to **1**, although the profile of the curve is different and can be simulated as a physical mixture of 3/2 (87%) and 1/2 (13%) spin systems. As a consequence, the magnetic behaviour of complexes **1**–**4** and **6** is very complicated and theoretical studies are required to provide a complete and satisfactory explanation.

On one hand, the magnetic properties of a particular Ru_2^{5+} species are a consequence of the separation energy of the π* and δ* orbitals. On the other hand, the electronic transitions where those orbitals are involved usually appear in the visible-near-infrared region. These facts suggest that there may be a relationship between the magnetic properties of a particular species and its electronic spectra. This relationship is especially interesting in this kind of diruthenium complex where a surprising variety of magnetic behaviours occur.[4,6–9] We have observed five different profiles in the electronic spectra of tris- and tetrakis(formamidinato)diruthenium complexes, which are related to their magnetic properties at room temperature (Table 1):

1) *High-spin complexes*: The usual high-spin configuration of Ru_2^{5+} complexes has been represented traditionally as $(\pi^*\delta^*)^3$ to show the near degeneracy of π* and δ* orbitals, although the exact order of the levels is not assured.[2] Two different profiles are obtained in the electronic spectra of these high-spin complexes (both in dichloromethane and in the solid state): i) One absorption in the range 512–531 nm with or without significant shoulders at lower energy[3,4,10] (profile **a**). ii) Two absorptions in the ranges 462–494 and 601–706 nm, sometimes with a small absorption between them[11,12] (profile **b**).

Table 1. Magnetic moment and electronic spectral data for formamidinate complexes of Ru_2^{5+}.

Compound	μ [BM]	Electronic absorptions [nm]
High-spin complexes		
$[Ru_2Cl(O_2CMe)(DPhF)_3]$	4.0[b]	528, ≈585, ≈685[a,c] 515, ≈565, ≈665[d,3]
$[Ru_2Cl(O_2CC_6H_5)(DPhF)_3]$	4.19[4]	519, ≈566, ≈662[d,4]
$[Ru_2Cl(O_2CC_6H_4OC_{10}H_{21})(DPhF)_3]$		517, ≈565, ≈665[d,4]
$[Ru_2Cl(O_2CC_6H_4CN)(DPhF)_3]\cdot H_2O$	4.15[4]	524, ≈570, ≈659[d,4]
$\{[Ru_2Cl(DPhF)_3(H_2O)]_2(O_2C)_2\}$	4.45[4]	532, ≈565, ≈660[d,4]
$\{[Ru_2Cl(DPhF)_3]_2(O_2C)_2C_6H_4\}\cdot 0.5\,H_2O$	4.18[4]	519, ≈558, ≈658[d,4]
$\{[Ru_2Cl(DPhF)_3]_3(O_2C)_3C_6H_3\}\cdot H_2O$	4.10[4]	514, ≈558, ≈656[d,4]
$\{[Ru_2(NCS)(DPhF)_3]_3(O_2C)_3C_6H_3\}$	3.91[4]	519, ≈589, ≈659[d,4]
$[Ru_2Cl(O_2CMe)(Dm\text{-}AniF)_3]$	3.72[10]	526[d,10]
$[Ru_2Cl(DPhF)_4]$	3.83[a]	465, 569, 704[a,c]
	3.83[12]	465, 570, 666[d,12]
	3.89[11]	462, 576, 666[d,11]
$[Ru_2Cl(Dm\text{-}MePhF)_4]$	[b,11]	
$[Ru_2Cl(Dp\text{-}ClPhF)_4]$	[b,11]	472, 583, 656[d,11]
$[Ru_2Cl(Dm\text{-}ClPhF)_4]$	[b,11]	475, 633[d,11]
$[Ru_2Cl(Dm\text{-}CF_3PhF)_4]$	[b,11]	473, 622[d,11]
$[Ru_2Cl(D3,4\text{-}Cl_2PhF)_4]$	[b,11]	489, 610[d,11]
$[Ru_2Cl(D3,5\text{-}Cl_2PhF)_4]$	[b,11]	494, 601[d,11]
$[Ru_2I_2(DPhF)_3]$	3.79[a]	560, ≈705, ≈910[a,d]
Low-spin complexes		
$[Ru_2(NCS)(O_2CMe)(DPhF)_3]$	1.7[b]	410, 529, ≈665, 820[a,d,4]
$[Ru_2(CN)(DPhF)_4]$	1.6[b]	420, 531, ≈665, 807[a,d]
Intermediate-spin complexes		
$[Ru_2Cl(Dp\text{-}AniF)_4]$	≈3.58[9]	471, 583, 688[d,11]
$[Ru_2Br_2(DPhF)_3]$	3.39[a]	489, ≈585, 706, ≈820[a,c] 490, ≈570, 667, ≈845[a,d]
$[Ru_2(NO_3)_2(DPhF)_3]$	3.28[a]	465, ≈550, ≈670[a,c] 520, ≈680 [a,d]
$\{[Ru_2(DPhF)_3(H_2O)]_3(O_2C)_3C_6H_3\}\ (SO_3CF_3)_3\cdot 2\,THF$	3.57[a]	≈492, 585[d,4]
$[Ru_2(O_2CMe)(DPhF)_3(H_2O)]BF_4\cdot 0.5\,CH_2Cl_2$	3.09[7]	≈485, 591, ≈632, ≈720[a,c] 495, 564 [d,7]
$[Ru_2Cl_2(DPhF)_3]$	2.71[a]	≈546, ≈625, 673, ≈810[a,d] ≈525, 624, ≈840[a,d]
$[Ru_2(BF_4)(DPhF)_3(H_2O)]BF_4\cdot THF$	2.55[a]	490, ≈570, 739, ≈845[a,c] 464, ≈545, ≈760[a,d]

[a] This work. [b] Magnetic moment between 3.64 and 3.97 BM. [c] In Nujol. [d] In dichloromethane.

Diruthenium complexes with three formamidinate ligands and one carboxylate ligand show the profile **a**, instead of the more electron-rich complexes with four formamidinates which show the profile **b**. Moreover, the chloridotetracarboxylatodiruthenium(II,III) complexes generally reveal only one maximum in the visible spectra (profile **a**), although two absorptions are also possible for electron-rich diruthenium species,[13,14] such as $[Ru_2I_2(O_2CMe)_4]^-$. Figure 3 shows, as an example, the electronic spectra in solution and in the solid state of $[Ru_2Cl(O_2CMe)(DPhF)_3]$ (profile **a**) and $[Ru_2Cl(DPhF)_4]$ (profile **b**).

2) *Low-spin complexes*: Only two low-spin Ru_2^{5+} complexes with formamidinate ligands have been described.[6] Both complexes show very similar electronic spectra with three maxima centred at about 400, 450, and 800 nm (profile **c**). Figure 4 shows the electronic spectra in solution of the low-spin complexes $[Ru_2(CN)(DPhF)_4]$ and $[Ru_2(NCS)(O_2CMe)(DPhF)_3]$.

3) *Intermediate-spin systems*: Among the complexes which have been described showing intermediate-spin situations, two different profiles can be distinguished in their electronic spectra: One similar to the profile **b** and another which presents one band near 600 nm and a shoulder at higher energy (profile **d**).

The electronic spectrum of complex **1** shows the profile **d** (Figure 5). The same profile was observed in the complexes $[Ru_2(O_2CMe)(DPhF)_3(H_2O)]BF_4\cdot 0.5\,CH_2Cl_2$[7] and $\{[Ru_2(DPhF)_3(H_2O)]_3(O_2C)_3C_6H_3\}(SO_3CF_3)_3\cdot 2\,THF$,[4] the magnetic behaviour of which has been explained as quantum mechanical and physical spin admixtures, respectively. The profile of the visible spectra of complex **5** is intermediate between the profiles **a** and **d**.

Complexes **2**, **3** and **6** have electronic spectra of the type **b** similar to the complex $[Ru_2Cl(Dp\text{-}AniF)_4]$.[9] These complexes presumably display magnetic behaviour corresponding to a Boltzmann distribution. The intermediate-spin state found for $[Ru_2Cl(Dp\text{-}AniF)_4]$ contrasts with the high-spin state showed by other tetrakis-

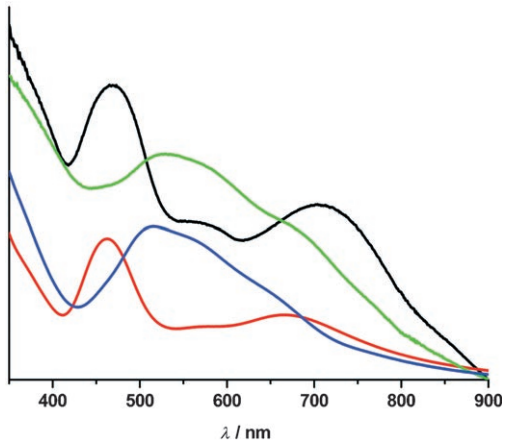

Figure 3. Typical profiles observed in the visible spectra of high-spin formamidinate complexes: $[Ru_2Cl(DPhF)_4]$ (black and red) and $[Ru_2Cl(O_2CMe)(DPhF)_3]$ (green and blue) in the solid state (up) and in dichloromethane solution (down).

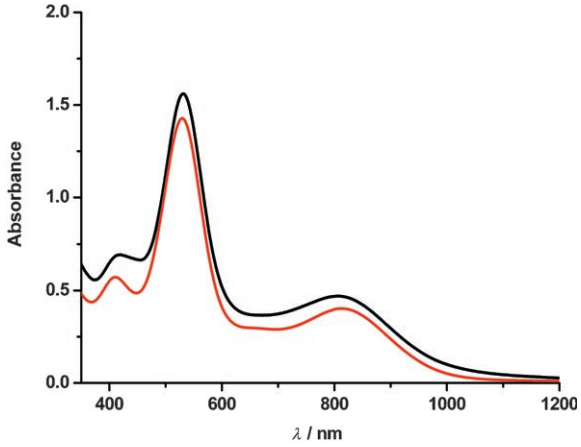

Figure 4. Visible spectra of the low-spin formamidinate complexes $[Ru_2(CN)(DPhF)_4]$ (black) and $[Ru_2(NCS)(O_2CMe)(DPhF)_3]$ (red) in dichloromethane solution.

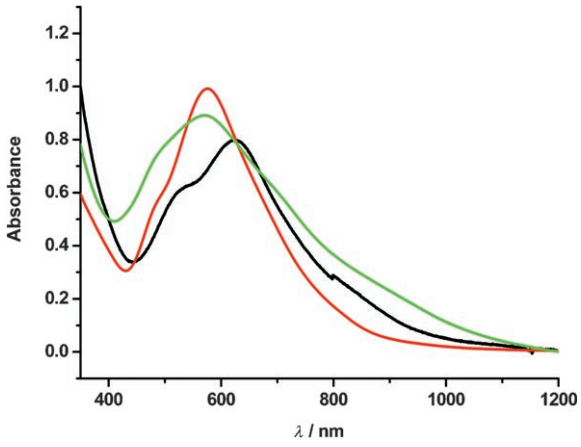

Figure 5. Visible spectra in dichloromethane solution of complex **1** (black), **5** (green) and $[Ru_2(O_2CMe)(DPhF)_3(H_2O)]BF_4$ (red).

(formamidinato)diruthenium derivatives, including the analogous complex $[Ru_2Cl(Dm\text{-}AniF)_4]$. Those data suggest that this last compound is at the frontier of the high-spin behaviour. Thus, a slightly more basic formamidinate is already capable of provoking the change. Complex **4** presents a similar electronic spectrum, although its magnetic moment curve corresponds to a physical mixture of spins. As expected, complexes **4** and **6** present notable differences between their visible spectra in the solid state and in dichloromethane solution probably due to the formation of other species in solution. Figure 6 shows the spectra in the solid state.

X-ray crystallography: The structures of compounds **2**, **4**·THF, and **6** are shown in Figures 7, 8 and 9, respectively. Selected bond lengths, angles, and torsion angles are presented in Table 2.

$[Ru_2Br_2(DPhF)_3]$ (**2**) consists of a paddlewheel arrangement where one of the paddles has been substituted by two terminal equatorial ligands (Figure 7). Similar structures

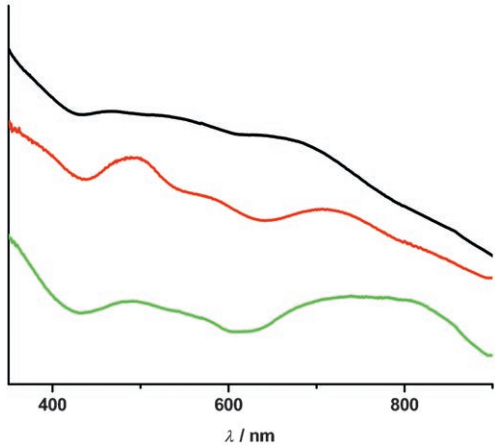

Figure 6. Vis-NIR spectra in the solid state (Nujol mulls) of **2** (red), **4**·THF (green) and **6** (black).

Table 2. Selected bond lengths [Å], angles [°], and torsion angles [°] for **2**, **4**·THF and **6**.

		2	
Ru1–Ru2	2.4011(6)	Ru2–N6	2.041(4)
Ru1–Br1	2.4827(7)	N1-Ru1-Br1	164.86(14)
Ru2–Br2	2.4836(7)	N2-Ru2-Br2	167.01(13)
Ru1–N1	2.017(4)	Br1-Ru1-Ru2-Br2	−3.61(3)
Ru1–N3	2.046(4)	N1-Ru1-Ru2-N2	−3.70(17)
Ru1–N5	2.039(4)	N3-Ru1-Ru2-N4	−2.24(17)
Ru2–N2	2.025(4)	N5-Ru1-Ru2-N6	−6.34(17)
Ru2–N4	2.033(4)		
		4·THF	
Ru1–Ru2	2.4108(9)	Ru1–F1	2.069(11)
Ru1–N1	2.049(11)	Ru2–F2	2.099(12)
Ru1–N2	1.969(14)	Ru1–O1	2.287(7)
Ru1–N3	1.978(14)	B1–F1	1.47(2)
Ru2–N4	2.074(13)	B1–F2	1.46(2)
Ru2–N5	1.972(15)	B1–F3	1.40(2)
Ru2–N6	2.005(14)	B1–F4	1.33(2)
		6	
Ru1–Ru2	2.3694(4)	Ru2–N6	1.998(3)
Ru1–N1	2.046(3)	Ru1–O1	2.334(2)
Ru1–N4	2.048(3)	Ru1–O2	2.123(2)
Ru1–N5	2.008(3)	Ru2–O4	2.116(2)
Ru2–N2	2.034(3)	Ru2–O5	2.378(3)
Ru2–N3	2.048(3)		

have been reported for other transition metals with triazenide bridging ligands: $[Mo_2Cl_2(R_2N_3)_3]$ (R = *p*-Tol, Ph)[15] and $[Tc_2Cl_2(R_2N_3)_3]$ (R = *p*-Tol).[16] However, as far as we are aware, there is no precedent of such a structure in ruthenium chemistry in any oxidation state. Moreover, this is the first example of a Ru_2^{5+} compound in which both axial positions are free of ligands, which, paradoxically, does not produce a short metal–metal bond (2.4011(6) Å). The large size of the two close bromide ligands can influence this distance. In fact, the angles N1-Ru1-Br1 (164.86(14)°) and N2-Ru2-Br2 (167.01(13)°) are far from linear. However, the structure is quite eclipsed (Table 2).

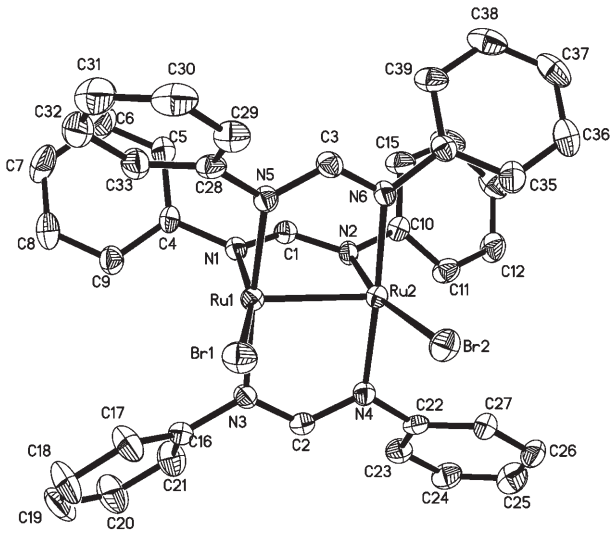

Figure 7. ORTEP view of the complex $[Ru_2Br_2(DPhF)_3]$ (**2**). Hydrogen atoms are omitted for clarity.

$[Ru_2(BF_4)(DPhF)_3(H_2O)]BF_4$·THF (**4**·THF) presents a paddlewheel arrangement with one axial position occupied by a water molecule (Figure 8) as compound $[Ru_2(O_2CMe)(DPhF)_3(H_2O)]BF_4$·$0.5\,CH_2Cl_2$ (d(Ru–Ru) = 2.3503(9) Å),[7] although in **4**·THF the metal–metal bond is longer (2.4108(9) Å). One BF_4^- group acts as a bridge between the ruthenium atoms. Among the few compounds in which BF_4^- bridges metal atoms, only two are discrete species: $[Cu_2F_2(mppzH)_4(BF_4)_2]$ (mppzH = 3-methyl-5-phenylpirazole)[17] and $\{CuF(BF_4)(tmen)\}_2$ (tmen = tetramethylethylenediamine).[18] The distances Cu–F in those examples are very long (2.502(5)–2.693(2) Å) and, therefore, the BF_4^- groups are considered as *semicoordinated*. However, in complex **4**·THF the Ru–F bond lengths are very short (2.069(11) and 2.099(12) Å) and comparable to the length found in several ruthenium complexes in which the fluoride is a terminal ligand: 2.069(2) Å in $[RuF(CO)(dppp)_2]PF_6$, 2.069(3) and 2.056(3) Å in $[Ru_2F_2(dppp)_2]$ (dppp = 1,3-bis(diphenylphosphino)propane),[19] or 2.065(1) Å in $[RuHF(CF_2)(CO)(PtBu_2Me)_2]$.[20] The strong ionic interaction between one BF_4^- and the electron-deficient unit $[Ru_2(DPhF)_3]^{2+}$ could explain the short lengths Ru–F in **4**·THF.[21] Nevertheless, the BF_4^- bridge is somehow activated as indicated by the long B–F lengths (Table 2). Electrophilic activation of BF_4^- upon coordination has been claimed for other complexes such as $[Fe(BF_4)(CO)(depe)_2]BF_4$ (depe = 1,2-bis(diethylphosphino)ethane)[22] or $[Mn(BF_4)(CO)_3(2\text{-}NMe_2\text{-}3\text{-}p\text{-}iPr_2\text{-}indene)]$.[23] A diruthenium(III) compound has also been reported in which two BF_4^- ligands are unidentate, coordinated to the axial positions, $[Ru_2(DMBA)_4(BF_4)_2]$ (DMBA = *N*,*N*′-dimethylbenzamidinate), with Ru–F lengths of 2.389(3) and 2.366(3) Å.[24] The other BF_4^- ligand in **4**·THF is linked through the F7 atom to the water axial ligand by a hydrogen bond.

Suitable crystals of $[Ru_2(DPhF)_3(MeCN)_2](BF_4)_2$ (**5**) for X-ray experiments were not obtained, but the structure of this complex is probably similar to the species $[Mo_2(DAniF)_3(MeCN)_2]^+$ (DAniF = *N*,*N*′-bis(*p*-anisyl)formamidinate),[25] which has been very useful for building higher nuclearity structures.[26,27]

The disposition of the formamidinate ligands in $[Ru_2(NO_3)_2(DPhF)_3]$ (**6**) is the same as that in **2** and **4**·THF. As shown above, in **2** neither of the axial positions are occupied, in **4**·THF one of them, and in **6** both positions are occupied (Figure 9). However, the metal–metal bond in **6** (2.3694(4) Å) is the shortest of the three (Table 2). Each nitrate group is coordinated to one ruthenium centre as chelate. The Ru–O bond lengths vary appreciably depending on the position, axial or equatorial. This interesting arrange-

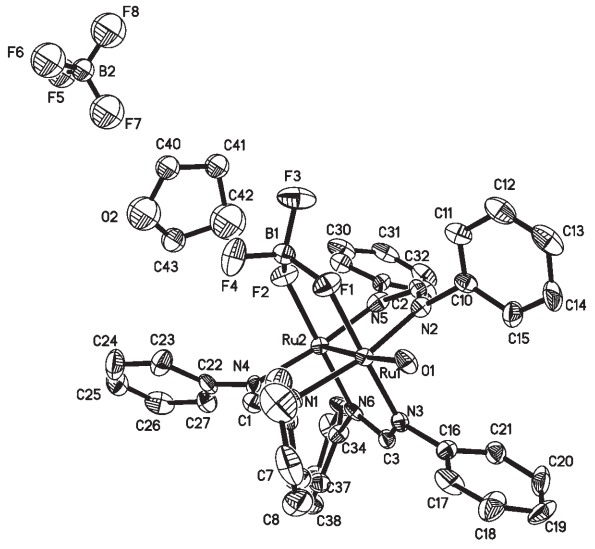

Figure 8. ORTEP view of the complex $[Ru_2(BF_4)(DPhF)_3(H_2O)]BF_4$·THF (**4**·THF). Hydrogen atoms and crystallisation solvent are omitted for clarity.

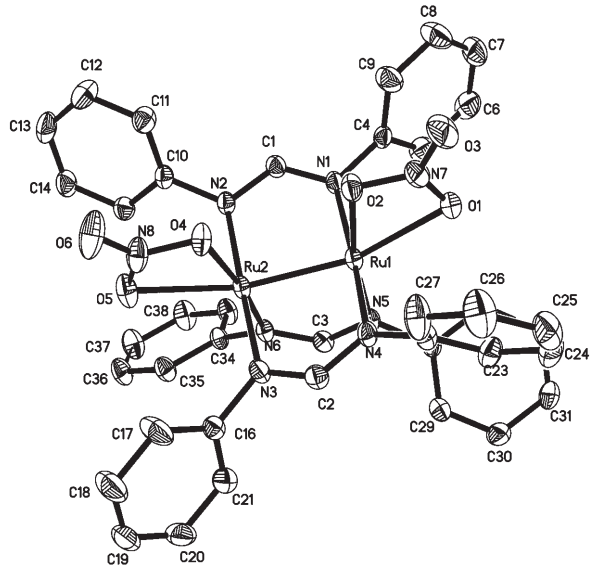

Figure 9. ORTEP view of the complex $[Ru_2(NO_3)_2(DPhF)_3]$ (**6**). Hydrogen atoms are omitted for clarity.

ment was already found for the compound $[Rh_2(NO_3)_2(DTolF)_3]$ (DTolF = *N*,*N*′-bis(*p*-tolyl)formamidinate).[28] However, there are very few ruthenium complexes in which NO_3^- acts as a chelate ligand,[29,30] and they are mononuclear compounds.

Conclusion

The chemical stability of the unit $[Ru_2(DPhF)_3]^{2+}$ has been previously observed for other carboxylatotris(dipheylformamidinato) complexes[4] of Ru_2^{5+}. The results reported here show how this fragment endures the presence of diluted hydracids. $[Ru_2(BF_4)(DPhF)_3(H_2O)]BF_4$·THF (**4**·THF) and $[Ru_2(DPhF)_3(MeCN)_2](BF_4)_2$ (**5**) are also probably good starting materials for preparing other dinuclear or polynuclear complexes thanks to the lability of their equatorial ligands. The inertia of the $[Ru_2(DPhF)_3]^{2+}$ group in such complexes also makes them good candidates to test catalytic reactions.

However, our main interest in these new diruthenium complexes is their usefulness to fully understand the variety of magnetic behaviours of this class of complexes and, especially, the relationship among their outstanding magnetic properties, their electronic absorptions, and structural features such as the peculiar dependence of their metal–metal bond lengths on temperature.[9] Although there are many factors that may influence the electronic spectra, we point out certain parallelism between the visible-near-infrared spectra and the magnetic behaviour of formamidinatodiruthenium complexes containing the Ru_2^{5+} unit. Theoretical calculations are needed to further clarify the situation.

Experimental Section

All reactions were carried out in air. Chemicals, including the hydracids HCl (35%), HBr (48%) and HI (47%), and solvents were purchased from commercial sources and used without further purification. $[Ru_2Cl(O_2CMe)(DPhF)_3]$,[3] $[Ru_2(NCS)(O_2CMe)(DPhF)_3]$,[6] $[Ru_2(CN)(DPhF)_4]$,[3] $[Ru_2Cl(DPhF)_4]$,[12] and $[Ru_2(O_2CMe)(DPhF)_3(H_2O)]BF_4$·0.5 CH_2Cl_2[7] were prepared by following reported procedures. The reactions with silver salts were carried out under exclusion of light. Elemental analyses were done by the Microanalytical Service of the Complutense University of Madrid. IR spectra were obtained with an FT Midac prospect spectrophotometer by using KBr pellets. Electronic spectra of the complexes in dichloromethane solution ($\approx 10^{-4}$ M) and in the solid state (Nujol mulls) were acquired by using a Cary 5G spectrophotometer. Variable-temperature magnetic susceptibility measurements were performed on a Quantum Design MPMSXL SQUID magnetometer. All data were corrected for the diamagnetic contribution to the susceptibility of both the sample holder and the compound. Molar diamagnetic corrections were calculated on the basis of the Pascal constants.

$[Ru_2Cl_2(DPhF)_3]$ (1): Hydrochloric acid (6 drops) was added to a suspension of $[Ru_2Cl(O_2CMe)(DPhF)_3]$ (0.430 g, 0.487 mmol) in MeOH (7 mL). After stirring for 1 h, the solid was filtered, washed with MeOH (6 × 2 mL), and dried under vacuum. Yield: 79%. IR (KBr): $\tilde{\nu}$ = 3060 w, 3034 w, 2953 w (ν(C–H)); 1591 m, 1582 m (ν(C=C)); 1525 vs, 1487 vs (ν(C=N)); 1320 s, 1213 vs (ν(C–N)); 1077 w, 1028 w (δ_{ip}(C=C–H)); 955 w, 935 m (δ(N=C–H)); 756 s, 693 cm^{-1} s (δ_{oop}(C=C–H)); UV/Vis-NIR (CH_2Cl_2): $\lambda_{max}(\varepsilon) = \approx 265$ (50000), ≈ 380 (3800), ≈ 525 (4000), 624 (6000), ≈ 840 nm (3000 mol^{-1} dm^3 cm^{-1}); Vis-NIR (Nujol): $\lambda_{max} = \approx 546$, ≈ 625, 673, ≈ 810 nm; $\mu_{eff} = 2.73\ \mu_B$ at room temperature; elemental analysis calcd (%) for $C_{39}H_{33}Cl_2N_6Ru_2$ (858.784): C 54.55, H 3.87, N 9.79; found: C 54.50, H 3.87, N 9.66.

$[Ru_2Br_2(DPhF)_3]$ (2): A fine precipitate of complex **2** was obtained after a slow addition of hydrobromic acid in excess (1 mL) to a suspension of $[Ru_2(O_2CMe)(DPhF)_3(H_2O)]BF_4$·0.5 CH_2Cl_2 (0.200 g, 0.201 mmol) in MeOH (10 mL). After the mixture had been stirred for 20 min, the solid was filtered, washed with MeOH (5 × 2 mL) and Et_2O (4 × 2 mL), and dried under vacuum. Yield: 81%. IR (KBr): $\tilde{\nu}$ = 3054 w, 3032 w, 2949 w (ν(C–H)); 1591 m, 1582 m (ν(C=C)); 1521 vs, 1486 vs (ν(C=N)); 1312 s, 1213 vs (ν(C–N)); 1079 w, 1027 w (δ_{ip}(C=C–H)); 952 w, 933 m (δ(N=C–H)); 757 s, 693 cm^{-1} s (δ_{oop}(C=C–H)); UV/Vis-NIR (CH_2Cl_2): $\lambda_{max}(\varepsilon) = \approx 300$ (13500), ≈ 385 (2800), 490 (3100), ≈ 570 (2250), 667 (2150), ≈ 845 nm (750 mol^{-1} dm^3 cm^{-1}); Vis-NIR (Nujol): $\lambda_{max} = \approx 390$, 489, ≈ 585, 706, ≈ 820, ≈ 1060 nm; $\mu_{eff} = 3.37\ \mu_B$ at room temperature; elemental analysis calcd (%) for $C_{39}H_{33}Br_2N_6Ru_2$ (947.696): C 49.43, H 3.51, N 8.87; found: C 50.10, H 3.54, N 9.00.

$[Ru_2I_2(DPhF)_3]$ (3): This compound was prepared similarly to **2** by using hydroiodic acid. Yield: 75%. IR (KBr): $\tilde{\nu}$ = 3053 w, 3030 w, 2954 w (ν(C–H)); 1588 m (ν(C=C)); 1519 vs, 1485 vs (ν(C=N)); 1316 s, 1212 vs (ν(C–N)); 1076 w, 1027 w (δ_{ip}(C=C–H)); 955 w, 934 m (δ(N=C–H)); 757 s, 693 cm^{-1} s (δ_{oop}(C=C–H)); UV/Vis-NIR (CH_2Cl_2): $\lambda_{max}(\varepsilon) = \approx 290$ (38500), ≈ 355 (18000), 560 (6500), ≈ 705 (5200), ≈ 910 nm (4000 mol^{-1} dm^3 cm^{-1}); Vis-NIR (Nujol): $\lambda_{max} = \approx 380$, 489, ≈ 585, 706, ≈ 820, ≈ 1060 nm; $\mu_{eff} = 3.79\ \mu_B$ at room temperature; elemental analysis calcd (%) for $C_{39}H_{33}I_2N_6Ru_2$ (1041.686): C 44.97, H 3.19, N 8.07; found: C 44.78, H 3.22, N 7.98.

$[Ru_2(BF_4)(DPhF)_3(H_2O)]BF_4$·THF (4·THF): $AgBF_4$ (0.117 g, 0.601 mmol) in THF (8 mL) was added to a suspension of **1** (0.250 g, 0.291 mmol) in THF (2 mL). The mixture was stirred overnight. The precipitate was filtered off by using Celite, and the resulting solution was layered with hexanes. Two weeks later, the crystals were collected. Yield: 45%. IR (KBr): $\tilde{\nu}$ = 3059 w, 2959 w, 2877 w (ν(C–H)); 1591 m, (ν(C=C)); 1522 s, 1487 vs (ν(C=N)); 1317 s, 1214 vs (ν(C–N)); 1077 w, 1028 w (δ_{ip}(C=C–H)); 1058 s (BF_4); 964 w, 939 m (δ(N=C–H)); 779 m; 762 s, 698 cm^{-1} s (δ_{oop}(C=C–H)); 521, 442 UV/Vis-NIR (CH_2Cl_2): $\lambda_{max}(\varepsilon) = \approx 285$ (32500), 464 (8000), ≈ 545 (6800), 637 (7000), ≈ 760 (5700), ≈ 1020 nm (2300 mol^{-1} dm^3 cm^{-1}); Vis-NIR (Nujol): $\lambda_{max} = \approx 330$, 490, ≈ 570, 739, ≈ 845, 1082 nm; $\mu_{eff} = 2.55\ \mu_B$ at room temperature; elemental analysis calcd (%) for $C_{43}H_{43}B_2F_8N_6O_2Ru_2$ (1051.61): C 49.11, H 4.12, N 7.99; found: C 49.37, H 4.19, N 8.05.

$[Ru_2(DPhF)_3(MeCN)_2](BF_4)_2$ (5): This complex was obtained from recrystallisation of **4** in MeCN/Et_2O. IR (KBr): $\tilde{\nu}$ = 3059 w, 2930 w (ν(C–H)); 2314 w, 2295 w, 2277 w (ν(C=N)); 1591 m, (ν(C=C)); 1533 s, 1487 vs (ν(C=N)); 1316 s, 1211 vs (ν(C–N)); 1077 w, 1028 w (δ_{ip}(C=C–H)); 1059 s (BF_4); 937 m (δ(N=C–H)); 779 m, 764 s, 697 s (δ_{oop}(C=C–H)); 538w, 454 cm^{-1} m; UV/Vis-NIR (CH_2Cl_2): $\lambda_{max}(\varepsilon) = \approx 485$ (5200), 570 (6700), ≈ 704 (4700), ≈ 916 nm (2050 mol^{-1} dm^3 cm^{-1}); Vis-NIR (Nujol): $\lambda_{max} = \approx 290$, ≈ 495, 586, ≈ 623, ≈ 689, ≈ 840 nm; elemental analysis calcd (%) for $C_{43}H_{39}B_2F_8N_8Ru_2$ (1043.593): C 49.49, H 3.77, N 10.74; found: C 49.45, H 3.90, N 10.86.

$[Ru_2(NO_3)_2(DPhF)_3]$ (6): This complex was isolated similarly to **4**·THF by using $AgNO_3$ instead of $AgBF_4$. Yield: 67%. IR (KBr): $\tilde{\nu}$ = 3059 w, 2951 w (ν(C–H)); 1592 m, (ν(C=C)); 1521 vs, 1487 vs (ν(C=N)); 1384 m, 1237 m, 996 m (ν(NO)); 1310 s, 1214 vs (ν(C–N)); 1074 w, 1026 w (δ_{ip}(C=C–H)); 939 m (δ(N=C–H)); 782 m, 760 s, 696 s (δ_{oop}(C=C–H)); 449 cm^{-1} m; UV/Vis-NIR (CH_2Cl_2): $\lambda_{max}(\varepsilon) = \approx 380$ (7500), 520 (9550), ≈ 680 nm (5700 mol^{-1} dm^3 cm^{-1}); Vis-NIR (Nujol): $\lambda_{max} = \approx 280$, ≈ 380, 465, ≈ 550, ≈ 670 nm; $\mu_{eff} = 3.22\ \mu_B$ at room temperature; elemental analysis calcd (%) for $C_{39}H_{33}N_8O_6Ru_2$ (911.887): C 51.37, H 3.65, N 12.29; found: C 51.34, H 3.73, N 11.92.

X-ray crystal structure analysis: Details of the data collection and crystal structure refinement correction for **2**, **4**·THF, and **6** are collected in Table 3. Representative crystals were mounted on a Bruker Smart-CCD diffractometer with graphite-monochromated $Mo_{K\alpha}$ (λ = 0.71073 Å) radiation. Data were collected, at 293(2) K, over a hemisphere of the reciprocal space by combination of three exposure sets. The cell parameters

Table 3. Crystallographic data for **2**, **4**·THF and **6**.

	2	**4**·THF	**6**
empirical formula	$C_{39}H_{33}Br_2N_6Ru_2$	$C_{43}H_{41}B_2F_8N_6O_2Ru_2$	$C_{39}H_{33}N_8O_6Ru_2$
formula weight	947.67	1049.58	911.87
crystal size [mm^3]	$0.24\times0.18\times0.13$	$0.06\times0.13\times0.20$	$0.18\times0.20\times0.34$
crystal system	orthorhombic	triclinic	triclinic
space group	$P2_12_12_1$	$P1$	$P\bar{1}$
a [Å]	12.4854(5)	10.0269(9)	10.0455(7)
b [Å]	16.4531(7)	10.5360(9)	13.6748(10)
c [Å]	17.9596(8)	12.1816(11)	16.2817(11)
α [°]	90	98.239(2)	79.0600(10)
β [°]	90	97.019(2)	81.8580(10)
γ [°]	90	115.193(2)	72.4520(10)
volume [Å^3]	3689.3(3)	1128.10(17)	2085.3(3)
Z	4	1	2
ρ_{calcd} [g cm^{-3}]	1.706	1.545	1.452
μ [mm^{-1}]	3.021	0.745	0.777
F(000)	1868	527	918
θ range [°]	1.68 to 29.02	1.73 to 25.00	1.28 to 25.00
index ranges	$-11<h<16$	$-11<h<11$	$-11<h<11$
	$-14<k<22$	$-12<k<6$	$-16<k<16$
	$-24<l<24$	$-14<l<14$	$-10<l<19$
collected reflns	35371	5941	10882
independent reflns	9152	4776	7196
completeness [%] to θmax	95.2	98.6	98.1
data/restraints/parameters	9151/0/442	4776/6/508	7196/0/496
$R1$	0.0369	0.0497	0.0340
$wR2$ (all data)	0.0987	0.1299	0.0716
largest diff peak/hole [e Å^{-3}]	0.621/−0.905	0.956/−0.794	0.310/−0.321

were refined by least-squares fit of all reflections collected. The structures were solved by direct methods and refined by the full-matrix least-squares methods against F^2 of all data. Calculations were performed with the aid of the SHELXS and SHELXL programs.[31,32] Final mixed refinement for complexes **2** and **6** was undertaken with anisotropic thermal parameters for the non-hydrogen atoms. For complex **4** the non-hydrogen atoms were also anisotropically refined with some exceptions. The BF_4^- groups and the THF solvent molecules were refined isotropically for three cycles whereas only the coordinates were refined in the last cycle. CCDC-640178 (**2**), CCDC-640178 (**4**·THF) and CCDC-640180 (**6**) contain the supplementary crystallographic data in this paper. These data can be obtained free of charge from the Cambridge Crystallographic Data Centre via www.ccdc.cam.ac.uk/data_request/cif.

Acknowledgement

We are grateful to the Ministerio de Educación y Ciencia and the Comunidad de Madrid (projects no. CTQ2005–00397 and S-0505-MAT-0303) for financial support.

[1] F. A. Cotton, N. F. Curtis, C. B. Harris, B. F. G. Johnson, S. J. Lippard, J. T. Mague, W. R. Robinson, J. S. Wood, *Science* **1964**, *145*, 1305.
[2] F. A. Cotton, C. A. Murillo, R. A. Walton, *Multiple Bonds Between Metal Atoms*, 3rd ed., Springer, New York, **2005**.
[3] M. C. Barral, S. Herrero, R. Jiménez-Aparicio, M. R. Torres, F. A. Urbanos, *Inorg. Chem. Commun.* **2004**, *7*, 42.
[4] M. C. Barral, T. Gallo, S. Herrero, R. Jiménez-Aparicio, M. R. Torres, F. A. Urbanos, *Inorg. Chem.* **2006**, *45*, 3639.
[5] V. M. Miskowski, M. D. Hopkins, J. R. Winkler, H. B. Gray in *Inorganic Electronic Structure and Spectroscopy* (Eds.: E. I. Solomon, A. B. P. Lever), Wiley, New York, **1999**, p. 343.
[6] M. C. Barral, R. González-Prieto, S. Herrero, R. Jiménez-Aparicio, J. L. Priego, E. C. Royer, M. R. Torres, F. A. Urbanos, *Polyhedron* **2004**, *23*, 2637.
[7] M. C. Barral, S. Herrero, R. Jiménez-Aparicio, M. R. Torres, F. A. Urbanos, *Angew. Chem.* **2005**, *117*, 309; *Angew. Chem. Int. Ed.* **2005**, *44*, 305.
[8] M. C. Barral, S. Herrero, R. Jiménez-Aparicio, M. R. Torres, F. A. Urbanos, unpublished results.
[9] P. Angaridis, F. A. Cotton, C. A. Murillo, D. Villagrán, X. Wang, *J. Am. Chem. Soc.* **2005**, *127*, 5008.
[10] W.-Z. Chen, T. Ren, *Organometallics* **2005**, *24*, 2660.
[11] C. Lin, T. Ren, E. J. Valente, J. D. Zubkowsky, E. T. Smith, *Chem. Lett.* **1997**, 753.
[12] J. L. Bear, B. Han, S. Huang, K. M. Kadish, *Inorg. Chem.* **1996**, *35*, 3012.
[13] M. C. Barral, R. González-Prieto, S. Herrero, R. Jiménez-Aparicio, J. L. Priego, M. R. Torres, F. A. Urbanos, *Polyhedron* **2005**, *24*, 239.
[14] M. C. Barral, R. González-Prieto, R. Jiménez-Aparicio, J. L. Priego, M. R. Torres, F. A. Urbanos, *Eur. J. Inorg. Chem.* **2004**, 4491.
[15] F. A. Cotton, G. T. Jordan IV, C. A. Murillo, J. Su, *Polyhedron* **1997**, *16*, 1831.
[16] F. A. Cotton, S. C. Haefner, A. P. Sattelberger, *Inorg. Chem.* **1996**, *35*, 7350.
[17] W. C. Velthuizen, J. G. Haasnoot, A. J. Kinneging, F. J. Rietmeijer, J. Reedijk, *J. Chem. Soc. Chem. Commun.* **1983**, 1366.
[18] D. A. Handley, P. B. Hitchcock, T. H. Lee, G. J. Leigh, *Inorg. Chim. Acta* **2001**, *316*, 59.
[19] P. Barthazy, R. M. Stoop, M. Wörle, A. Togni, A. Mezzetti, *Organometallics* **2000**, *19*, 2844.
[20] D. Huang, P. R. Koren, K. Folting, E. R. Davidson, K. G. Caulton, *J. Am. Chem. Soc.* **2000**, *122*, 8916.
[21] C. Becker, I. Kieltsch, D. Broggini, A. Mezzetti, *Inorg. Chem.* **2003**, *42*, 8417.
[22] S. E. Landau, R. H. Morris, A. J. Lough, *Inorg. Chem.* **1999**, *38*, 6060.
[23] J. Cipot, D. Wechsler, R. McDonald, M. J. Ferguson, M. Stradiotto, *Organometallics* **2005**, *24*, 1737.
[24] G.-L. Xu, C. G. Jablonski, T. Ren, *Inorg. Chim. Acta* **2003**, *343*, 387.
[25] F. A. Cotton, J. P. Donahue, C. A. Murillo, *J. Am. Chem. Soc.* **2003**, *125*, 5436.
[26] F. A. Cotton, J. P. Donahue, C. A. Murillo, *Inorg. Chem.* **2001**, *40*, 2229.
[27] F. A. Cotton, L. M. Daniels, J. P. Donahue, C. Y. Liu, C. A. Murillo, *Inorg. Chem.* **2002**, *41*, 1354.
[28] P. Piraino, G. Bruno, F. Nicolo, F. Faraone, S. L. Schiavo, *Inorg. Chem.* **1985**, *24*, 4760.
[29] J. W. Steed, D. A. Tocher, *Polyhedron* **1994**, *13*, 167.
[30] P. Ghosh, A. Chakravorty, *Inorg. Chem.* **1997**, *36*, 64.
[31] G. M. Sheldrick, SHELXS-97, Program for the Solution of Crystal Structures, University of Göttingen, Göttingen (Germany), **1997**.
[32] G. M. Sheldrick, SHELXL-97, Program for the Solution of Crystal Structures, University of Göttingen, Göttingen (Germany), **1997**.

Received: March 29, 2007
Revised: June 29, 2007
Published online: September 28, 2007

